materials proceedings

MDPI

Proceeding Paper

Preparation of Mesoporous Bicrystalline N-Doped TiO_2 Nanomaterials for Sustainable RhB Degradation under Sunlight †

Elias Assayehegn [1,2,*] and Abraha Tadese Gidey [1,*]

[1] Department of Chemistry, Mekelle University, Mekelle P.O. Box 231, Ethiopia
[2] Materials Science and Technology Division, National Institute for Interdisciplinary Science and Technology (CSIR-NIIST), Thiruvananthapuram 695019, India
* Correspondence: assaye98@gmail.com (E.A.); abraha.tadesse@mu.edu.et (A.T.G.); Tel.: +251-979406226 (E.A.)
† Presented at the 4th International Online Conference on Nanomaterials, 5–19 May 2023; Available online: https://iocn2023.sciforum.net.

Abstract: N-doped titanium dioxide (N/TiO_2) nanomaterials were successfully prepared using titanium butoxide and guanidinium chloride by simple sol-gel method. The significance of annealing gas environment (air, argon, and nitrogen) on their physicochemical and photocatalytic degradation properties was investigated. Indeed, the gas type governed the crystal/phase nature from monophase anatase with less crystallinity to dual-phase anatase/rutile with higher crystallinity. Moreover, results revealed that the introduction of N in the TiO_2 matrix led to a red shift towards visible-light, narrowed the bandgap (2.35 eV), and suppressed recombination. Nobly, the N/TiO_2 prepared in air demonstrated the highest RhB degradation performance (99%) with the highest rate constant (0.0158 min^{-1}) which is twice faster than the undoped TiO_2.

Keywords: doping; TiO_2; photocatalysis; rhodamine B; anatase and rutile; wastewater; degradation

Citation: Assayehegn, E.; Gidey, A.T. Preparation of Mesoporous Bicrystalline N-Doped TiO_2 Nanomaterials for Sustainable RhB Degradation under Sunlight. *Mater. Proc.* **2023**, *14*, x. https://doi.org/10.3390/xxxxx
Published: 5 May 2023

Copyright: © 2023 by the authors. Submitted for possible open access publication under the terms and conditions of the Creative Commons Attribution (CC BY) license (https://creativecommons.org/licenses/by/4.0/).

1. Introduction

Sadly, due to rapid urbanization and industrialization, a growing number of toxic contaminants are entering to water bodies and the trend is expected to be worsened. For instance, RhB is one of the most ubiquitous and industrial effluents. It is particularly challenging and dangerous to degrade by deploying conventional techniques, since it is a hazardous and generates carcinogenic species [1,2]. Meanwhile, advanced oxidation process techniques (such as heterogeneous-catalysis, photocatalysis, electrochemical oxidation, and Fenton) have played indispensable role in neutralizing such dyes [3,4]. Particularly owing to its high chemical inertness, strong oxidizing power, and abundance, TiO_2 remains a promising photocatalyst in tackling such environmental problems [5].

Unfortunately, its large bandgap, low solar conversion, and high charge carrier recombination rate limit its practical applications [6], and in alleviating these problems, considerable researches have been carried out [7]. Among nonmetal doping, N-doping into TiO_2 matrix has gained specific attention; consequently, various N/TiO_2 nanostructures have proven better catalytic performance than typical TiO_2 under visible-light [8]. To suppress the charge recombination, preparing mixed-phase TiO_2 is recommended than its monophasic nanostructure, since the former materials have demonstrated a better photocatalytic performance [9]. However, preparing these mixed-phase nanomaterials requires high temperature (>600 °C) and follows multistep reactions; especially for brookite counterpart is quite challenging [7]. The disadvantage of such high temperature synthesis method is that it significantly reduces the active surface area of the catalyst. Thus,

preparing phase-heterojunction N/TiO_2 at lower energy still remains imperative. With this aim, in current work, the effect of annealing gas type on the physicochemical properties of N/TiO_2 was investigated. Variety of N/TiO_2 nanocrystals were synthesized via sol-gel method using guanidinium chloride (GUA) as an eco-friendly N-dopant source and characterized via different techniques. Besides, their RhB photodegradation performance under direct sunlight was explored.

2. Materials and Method

2.1. Synthesis of N/TiO_2 Nanocatalysts

The nanomaterials were prepared through our previous modified method [10,11]; typically:

- Titanium butoxide (11.4 mmol, Sigma Aldrich) was added into ethanolic solution (30 mL, ethanol/water 5:1) step-wise while vigorously stirring.
- In another beaker, equimolar amount of guanidinium chloride (98%, Sigma Aldrich) was added to a solution of ethanol (10 mL) and 5 drops of conc. HNO_3 while stirring.
- To this solution, the above white solution was added step-wise while stirring for 2 h.
- The resultant mixture was then sealed and aged for 12 days.
- Finally, it was heated at 400 °C for 4 h in a furnace under different gas environment with flow rate of 150 cm^3/min (Table 1). The samples prepared in atmospheric air, Ar, and N_2 were denoted as NT-A, NT-Ar, and NT-N, respectively. Following the same procedure, a control sample was prepared in air without adding N-dopant, designated as N-0.

Table 1. Synthesis parameters and XRD results of as-obtained photocatalysts.

Catalyst	$Ti(OBu)_4$ (mmol)	GUA (mmol)	Temp. (°C)	Gas Type	Phase Comp. (%)		Crystal Size (nm)	
					Anatase	Rutile	Anatase$^{(101)}$	Rutile$^{(110)}$
N-0	11.4	0	400	Air	96	4	9.3	-
NT-Ar		11.4		Argon	98	2	8.5	-
NT-N		11.4		Nitrogen	98	2	8.5	-
NT-A		11.4		Air	53	44	10.2	36.3

2.2. Characterization Techniques of Catalysts

The following techniques have been deployed: X-ray diffractometer (Bruker D8 Advance, Cu-Kα), field emission scanning electron microscopy (FESEM) (SEM (Quanta 400 FEG SEM)), photoluminescence, PL, (JASCO FP-6500), and Jasco V-650 spectrophotometer for the UV-Vis diffused reflectance (DRS).

2.3. Photocatalysis Study

Under natural sunlight, the experiments were carried out at CSIR-NIIST, Trivandrum- India in January. In typical study, as-synthesized photocatalyst (50 mg) was dispersed to RhB solution (200 mL, 20 mg L^{-1}). The dye-catalyst suspension was magnetically stirred for 30 min in the dark; it was then exposed to direct sunlight irradiation (11 am to 4 pm) while stirring. At a regular time interval, aliquots of the suspension were withdrawn. After removing the catalysts by centrifugation, the solution was analyzed by UV-vis spectrophotometer (UV-2401-PC-Shimadzu).

3. Results and Discussion

3.1. Structural Analysis

Figure 1 depicts the XRD patterns of as-prepared materials. It can be clearly seen that both NT-Ar and NT-N have 98% anatase phase (JCPDS: 21-1272) like N-0; whereas NT-A

comprises a mixture of 53% anatase and 44% rutile phases (JCPDS: 21-1276) with trace amount of brookite (Table 1) [12]. Comparing their respective XRD peaks, the doping occurred without changing the crystal structure in case of NT-Ar and NT-N; however, it caused a significant phase change in NT-A. Moreover, this difference in gas environment influences the degree of crystallinity and particle size; NT-A displays the highest crystallinity nature of all as-synthesized powders wth larger anatase nanoparticles size (10.2 nm) than that of NT-Ar and NT-N (8.5 nm) (Table 1). This strongly suggests that calcining TiO_2 nanoparticles in atmospheric air favors particle growth; while in Ar, and N_2 hinder the growth of the nanoparticles.

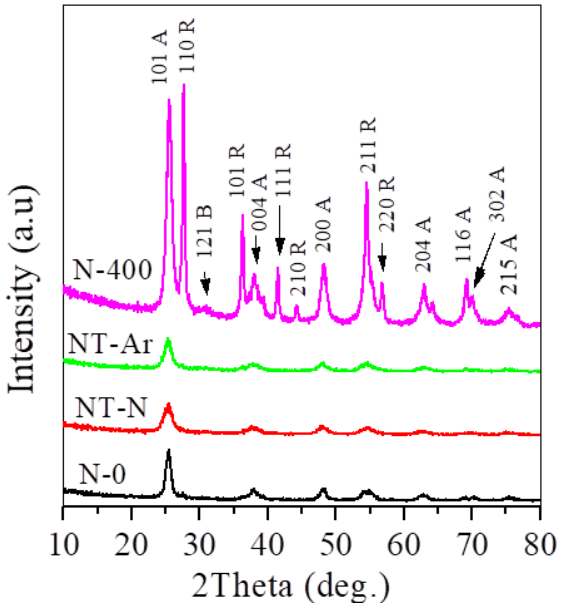

Figure 1. XRD data of as-prepared nanomaterials (A: anatase, R: rutile).

3.2. Morphological Analysis

The field-emission SEM images and elemental analysis of TiO_2 based materials are presented (Figure 2). The undoped has roughly spherical particles with aggregates (Figure 2a). Importantly, both NT-Ar and NT-N doped samples (Figure 2b,c) have spherical shape which infers to their surface stability by respective gas type. Whereas NT-A has coral-like structure (Figure 2d); in this particular sample, particle coarsening and neck formation among the particles are exhibited due to the surface energy increment under annealing in air. Consequently, its particle size is increased, which is in agreement with the previous XRD discussion. Meanwhile, according to EDAX elemental results (Figure 2e–h), N-0 has Ti and O, however the N/TiO_2 materials have a third additional N element with 6.8–10.1 atomic % range, confirming nitrogen has been effectively incorporated. Moreover, the figure also revealed that the doped-N is homogenously distributed.

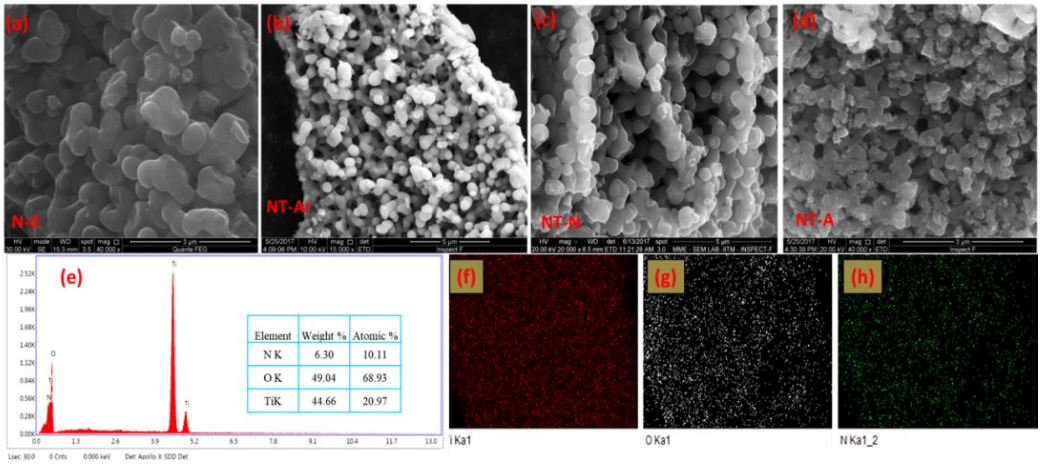

Figure 2. FESEM images of N-0 (**a**), NT-Ar (**b**), NT-N (**c**), NT-A (**d**); and EDAX of NT-A (**e**) with its elemental mapping of Titanium (**f**), Oxygen (**g**), Nitrogen (**h**).

3.3. Optical-Response Analysis

The DRS, Kubelka-Munk, and PL measurements of N-0, NT-Ar, NT-N, and NT-A are depicted (Figure 3); as shown, the unmodified white TiO_2 has an absorption peak in the UV region (~400 nm). However, all as-obtained N-doped catalysts have two peaks: a sharp peak at ~420 nm and abroad one in the range 420–600 nm, displaying an extended red shift to visible-light region. Meanwhile according Kubelka-Munk plot (Figure 3b), all the N/TiO_2 materials exhibited lower band gap energy (E_g) than TiO_2; NT-N particularly demonstrated the lowest E_g of 2.35 eV. Thus, incorporating N in the TiO_2 matrix not only led to a red shift (towards visible light) but also narrowed the band gap.

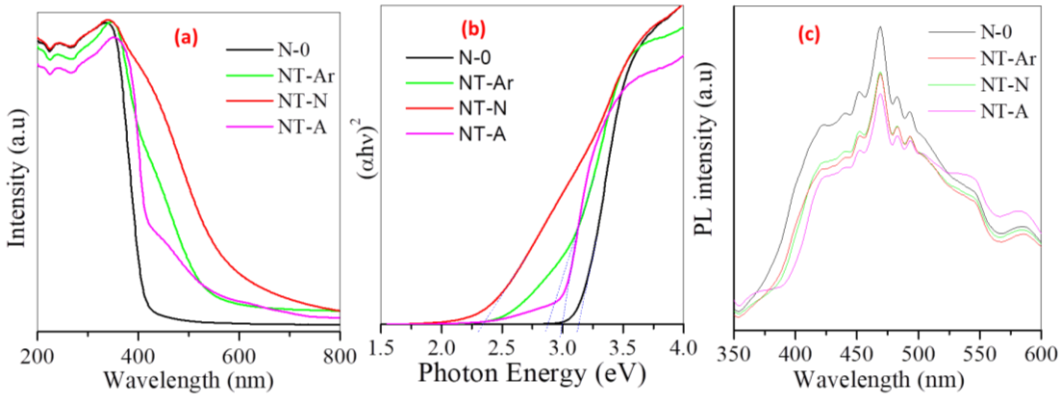

Figure 3. (**a**) DRS spectra; (**b**) Tauc plot; (**c**) PL spectra of as-obtained TiO_2 and N/TiO_2 nanomaterials.

Understanding how N-doping into the TiO_2 structure affects the rate of excitons is crucial; the PL spectra of the as-prepared materials are illustrated (Figure 3c). It is noted that all the doped materials exhibited a lower PL intensity in the range of 350–550 nm than unmodified sample, N-0. Displaying lower PL value by N/TiO_2 means they have lower charge carrier recombination rates which subsequently leads to high accessible e^-/h^+ density. Particularly, NT-A has recorded the lowest PL intensity due to the A/R heterojunction through which the e^-/h^+ can be easily separated unlike the other monoanatase phase. Consequently, this visible light-active material could perform better photocatalytic activity.

3.4. Evaluation of Sunlight-Driven Degradation

RhB has become a common deleterious environmental pollutant. As shown (Figure 4a,b), the concentration and characteristic RhB peak intensity are reduced as the function

of irradiation time. Particularly, NT-A displayed the highest photocatalytic efficiency, 99%, within 300 min sunlight irradiation (Figure 4c). It is noted that the RhB degradation performance was in the following order: NT-A > NT-N > N-0 > NT-Ar. Moreover, according to the photodegradation kinetics (Figure 4d), NT-A had the highest apparent rate constant (0.0158 min^{-1}) which is twice of the bare TiO_2. Such enhanced RhB decolouration over NT-A surface is ascribed to its higher degree of crystallinity, formation of A/R heterojunctions, lower recombination rate and higher accessible e^-/h^+ density, and higher aqueous-disperse character.

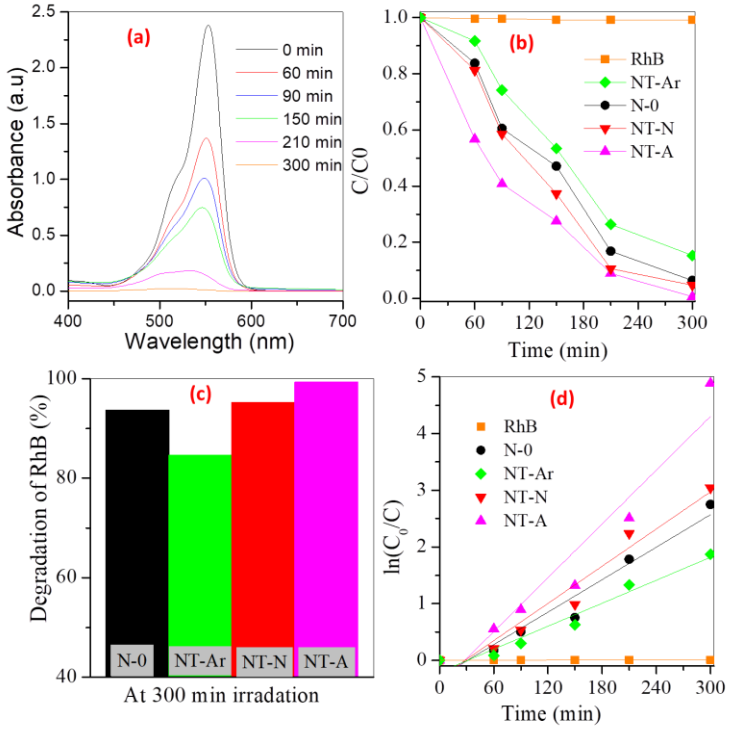

Figure 4. (**a**) UV-Vis spectra of RhB solutions after their respective irradiation time over NT-A; (**b**) RhB degradation rate under sunlight; (**c**) RhB photodegradation performance under 300 min irradiation; and (**d**) pseudo first order of as-synthesized catalysts.

4. Conclusions

Visible active N-doped titania nanomaterials were successfully prepared via sol-gel method using guanidinium chloride as N-source. The N/TiO_2 powders were optimized at different annealing gas types (air, argon, nitrogen) which profoundly influenced their physicochemical and photocatalytic properties. Among the variety as-obtained photocatalysts, the N/TiO_2 annealed in air displayed the highest RhB degradation performance (99%) within 5 hrs sunlight irradiation. This improved catalytic activity is mainly ascribed to the N-introduction into TiO_2 structure that led to higher crystallinity, optimal anatase/rutile phase composition, and well separated charge carriers.

Author Contributions:.

Funding: This research was funded by The World Academy of Sciences, Italy (CSIR-TWAS, FR No.: 3240293587), The Centre for Science & Technology of the Non-aligned and Other Developing Countries, India (RTF-DCS, No. NAM-05/74/16), and Mekelle University, Ethiopia (PG/CNCN/PhD/MU-NMBU/024/2019).

Acknowledgments: The authors express their sincere acknowledges to CSIR-NIIST, IIT Madras, Ethiopian Ministry of Education, and Mekelle University.

Conflicts of Interest: The authors declare no conflict of interest.

References

1. Hira, S.A.; Yusuf, M.; Annas, D.; Hui, H.S.; Park, K.H. Biomass-Derived Activated Carbon as a Catalyst for the Effective Degradation of Rhodamine B dye. *Processes* **2020**, *8*, 926.
2. Ismail, M.; Khan, M.I.; Khan, S.B.; Akhtar, K.; Khan, M.A.; Asiri, A.M. Catalytic reduction of picric acid, nitrophenols and organic azo dyes via green synthesized plant supported Ag nanoparticles. *J. Mol. Liq.* **2018**, *268*, 87–101. https://doi.org/10.1016/j.molliq.2018.07.030.
3. Zhang, B.; Li, X.; Ma, Y.; Jiang, T.; Zhu, Y.; Ren, H. Visible-light photoelectrocatalysis/H_2O_2 synergistic degradation of organic pollutants by a magnetic Fe_3O_4@SiO_2@mesoporous TiO_2 catalyst-loaded photoelectrode. *RSC Adv.* **2022**, *12*, 30577–30587. https://doi.org/10.1039/d2ra05183d.
4. Ahmed, M.A.; Adel, M. Recent progress in semiconductor/graphenephotocatalysts: Synthesis, photocatalytic applications, and challenges. *RSC Adv.* **2023**, *13*, 421–439. https://doi.org/10.1039/d2ra07225d.
5. Sudrajat, H.; Babel, S.; Ta, A.T.; Nguyen, T.K. Mn-doped TiO_2 photocatalysts: Role, chemical identity, and local structure of dopant. *J. Phys. Chem. Solids* **2020**, *144*, 109517. https://doi.org/10.1016/j.jpcs.2020.109517.
6. Kumaravel, V.; Rhatigan, S.; Mathew, S.; Bartlett, J.; Nolan, M.; Hinder, S.J.; Sharma, P.K.; Singh, A.; Byrne, J.A.; Harrison, J.; et al. Indium-Doped TiO_2 Photocatalysts with High-Temperature Anatase Stability. *J. Phys. Chem. C* **2019**, *123*, 21083–21096. https://doi.org/10.1021/acs.jpcc.9b06811.
7. Wu, J.; Feng, Y.; Logan, B.E.; Dai, C.; Han, X.; Li, D.; Liu, J. Preparation of Al-O-Linked Porous-g-C_3N_4/TiO_2-Nanotube Z-Scheme Composites for Efficient Photocatalytic CO_2 Conversion and 2,4-Dichlorophenol Decomposition and Mechanism. *ACS Sustain. Chem. Eng.* **2019**, *7*, 15289–15296. https://doi.org/10.1021/acssuschemeng.9b02489.
8. Nguyen, T.P.; Tran, Q.B.; Ly, Q.V.; Hai, L.T.; Le, D.T.; Tran, M.B.; Ho, T.T.T.; Nguyen, X.C.; Shokouhimehr, M.; Vo, D.V.N.; et al. Enhanced visible photocatalytic degradation of diclofen over N-doped TiO_2 assisted with H_2O_2: A kinetic and pathway study. *Arab. J. Chem.* **2020**, *13*, 8361–8371. https://doi.org/10.1016/j.arabjc.2020.05.023.
9. Zhao, C.; Wang, Z.; Chen, X.; Chu, H.; Fu, H.; Wang, C.C. Robust photocatalytic benzene degradation using mesoporous disk-like N-TiO_2 derived from MIL-125(Ti). *Chin. J. Catal.* **2020**, *41*, 1186–1197. https://doi.org/10.1016/S1872-2067(19)63516-3.
10. Assayehegn, E.; Solaiappan, A.; Chebudie, Y.; Alemayehu, E. Influence of temperature on preparing mesoporous mixed phase N/TiO_2 nanocomposite with enhanced solar light photocatalytic activity. *Front. Mater. Sci.* **2019**, *13*, 352–366. https://doi.org/10.1007/s11706-019-0481-0.
11. Assayehegn, E.; Solaiappan, A.; Chebude, Y.; Alemayehu, E. Fabrication of tunable anatase/rutile heterojunction N/TiO_2 nanophotocatalyst for enhanced visible light degradation activity. *Appl. Surf. Sci.* **2020**, *515*, 145966. https://doi.org/10.1016/j.apsusc.2020.145966.
12. Sadeghzadeh-Attar, A. Photocatalytic degradation evaluation of N-Fe codoped aligned TiO_2 nanorods based on the effect of annealing temperature. *J. Adv. Ceram.* **2020**, *9*, 107–122. https://doi.org/10.1007/s40145-019-0353-1.

Disclaimer/Publisher's Note: The statements, opinions and data contained in all publications are solely those of the individual author(s) and contributor(s) and not of MDPI and/or the editor(s). MDPI and/or the editor(s) disclaim responsibility for any injury to people or property resulting from any ideas, methods, instructions or products referred to in the content.